Available online at www.sciencedirect.com
ScienceDirect
Trans. Nonferrous Met. Soc. China 22(2012) 2517−2522
Transactions of Nonferrous Metals Society of China
www.tnmsc.cn

Ultrasonic synthesis of CoO/graphene nanohybrids as high performance anode materials for lithium-ion batteries

CHEN Bing-di[1, 2], PENG Cheng-xin[1, 2], CUI Zheng[2]

1. School of Materials Science and Engineering, Tongji University, Shanghai 201804, China;
2. Institute for Advanced Materials and Nano Biomedicine,
College of Medicine, Tongji University, Shanghai 200092, China

Received 9 July 2012; accepted 7 August 2012

Abstract: A facile ultrasonic method was used to synthesize CoO/graphene nanohybrids by employing $Co_4(CO)_{12}$ as a cobalt precursor. The nanohybrids were characterized by SEM, TEM and XPS, and the results show that CoO nanoparticles (3−5 nm) distribute uniformly on the surface of graphene. The CoO/graphene nanohybrids display high performance as an anode material for lithium-ion battery, such as high reversible lithium storage capacity (650 mA·h/g after 50 cycles, almost twice that of commercial graphite anode), high coulombic efficiency (over 95%) and excellent cycling stability. The extraordinary performance arises from the structure of the nanohybrids: the nanosized CoO particles with high dispersity on conductive graphene substrates are beneficial for lithium-ion insertion/extraction, shortening diffusion length for lithium ions and improving conductivity, thus the lithium storage performance was improved.

Key words: lithium-ion battery; graphene; CoO; anode material; ultrasonic synthesis

1 Introduction

Lithium-ion batteries (LIBs) have attracted considerable attention due to their high electromotive force and high energy density as a power source for portable electron devices and the large-scale electric application [1−3]. Graphite is usually employed as a commercial anode material for LIBs with a theoretical capacity of 374 mA·h/g. However, to meet the increasing demand for advanced lithium ion batteries, especially their potential applications in electrical/hybrid vehicles, many efforts have been made to explore the alternative electrode materials with high energy density and good rate capability [4].

Recently, graphene-based materials have attracted much attention for promising alternative anode materials in LIB [5−8]. These composites consist of graphene and metal oxides or their derivation, such as SnO_2/SnS_2/$SnSe_2$, Co_3O_4/CoO, Fe_3O_4/Fe_2O_3, Mn_3O_4, NiO/$Ni(OH)_2$, CuO/Cu_2O, TiO_2/$Li_4Ti_5O_{12}$ to enhance reversible capacity and rate capability [9−17]. In these composites, metal oxides are distributed on the surface of graphene or between the graphene layers, which can not only provide the high lithium storage capacity (>600 mA·h/g), but also effectively reduce the degree of the restacking of graphene and expose more active surface area to the electrolytes [10,18]. The superior electric conductive graphene can greatly improve the transportation of the electron of the whole electrode [12−15,19]. Moreover, graphene can be used as host matrix to buffer the volume change of the metal oxides during the charge/discharge processes, which successfully suppressed the decay of cycling performance of LIB [20−22]. Nevertheless, the preparation routes, such as one-pot chemical reduction of metal oxides/graphene composites and assembly of the metal oxides onto graphene nanosheets via multi-step methods, have less manipulation on the dispersion of the metal oxides and graphene [14,23−25], thus graphene has a tendency to restack and therefore affects the distribution of the metal oxides on the graphene matrix during the preparation of the composite processes.

In this work, we present a ultrasonic strategy to

Foundation item: Project (4340142501) supported by Start-up Funds of Chair Professor, Tongji University, China; Project (51173135) supported by the National Natural Science Foundation of China
Corresponding author: PENG Cheng-xin; Tel: +86-21-65983706; E-mail: pchxxm@126.com
DOI: 10.1016/S1003-6326(11)61494-5

prepare the nanosized CoO/graphene composites and evaluate their electrochemical performance for LIB. During the ultrasonic processes, graphene can be completely dispersed and serve as the electric conductive support for the metal oxides, while cobalt monoxide (CoO) nanoparticles firmly adhere to the surface of graphene or are surrounded by the flexible graphene nanosheets. Such three-dimensional metal oxides/ graphene composites are advantageous for inhibiting aggregation and volume change of CoO nanoparticles during cycling and offer a short diffusion path of lithium ion. Thus, as expected, the CoO/graphene composites exhibit a high reversible lithium storage capacity as an anode material for LIB.

2 Experimental

Nanosized CoO/graphene composites were prepared by a ultrasonic method at room temperature. Graphene nanosheets were obtained by the rapid exfoliation of graphite oxide at a low temperature using the previous method. $Co_4(CO)_{12}$ was purchased from Alfa Aesar China (Tianjin) Co., Ltd. The experimental details were described as follows: 40 mg graphene nanosheets were dispersed in 90 mL hexane by sonicate for 1 h, then an appropriate quantity of $Co_4(CO)_{12}$ was directly added into the above solution by sonicate for an additional 1 h. After the reaction completed, the resulted products were centrifugalized, washed with deionized water and ethanol to remove possibly remaining ions in the final product, and dried at 60 °C in air.

The morphology of the product was characterized by scanning electron microscopy (SEM, JEOL, JSM−6700F) and transmission electron microscopy (TEM, JEOL, JSE−2100F). The chemical composites of the product were determined by X-photoelectron spectroscopy (XPS, PHI 5000C ESCA System).

Electrochemical performance was evaluated via a CR2016-type coin cell on a LAND battery test system (CT2001A, Wuhan, China). The working electrode was composed of 80% active material (CoO/graphene composites), 12% acetylene black (Super-P), and 8% poly(vinylidene fluoride) (PVDF) binder dissolved in N-methyl-2-pyrrolidinone (NMP). Lithium foils were used as the counter and reference electrode, and polypropylene (PP) membrane (Celgard 2400) was employed as a separator. The electrolytes were 1 mol/L $LiPF_6$ dissolved in a mixture of ethylene (EC) and diethyl carbonate (DEC) (1:1, in volume ratio). The batteries were assembled in an argon-filled glove-box and charged/discharged at various current densities of 50−500 mA/g in the fixed voltage range of 3.00−0.01 V at room temperature.

3 Results and discussion

The CoO/graphene composites were prepared under an ultrasonic condition at room temperature (see Fig. 1). Here, we used the metal carboxylic $Co_4(CO)_{12}$ cluster as the precursors. Firstly, $Co_4(CO)_{12}$ cluster can be readily decomposed to metals Co and CO, as shown in reaction 1. Secondly, the active metal Co can be oxidized rapidly to CoO with the oxygen contained in the solutions, as illustrated in reaction 2. Thirdly, with the extension of the reaction time, nanosized CoO with positive charge can firmly adhere to the support of graphene with unsaturated p-π bonds due to the electrostatic attraction. While graphene can be effectively dispersed under the ultrasonic conditions, and expose more active surface area serving as the support for the metal oxides.

$$Co_4(CO)_{12} \rightarrow 4Co + 12CO \quad (1)$$

$$2Co + O_2 \rightarrow 2CoO \quad (2)$$

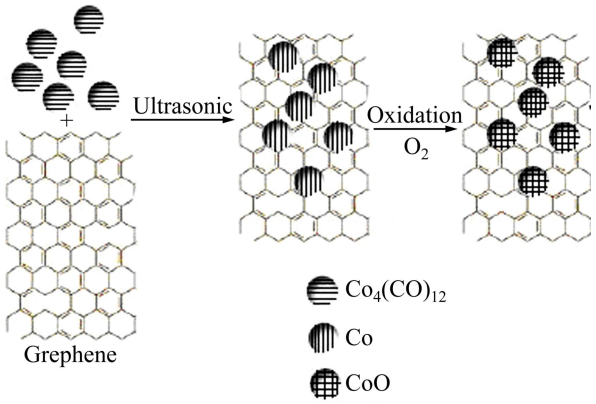

Fig. 1 Schematic illustration for ultrasonic synthesis of CoO/graphene nanohybrids

The morphology of the CoO/graphene composites is shown in Fig. 2(a). The overall sample was dominated by the three-dimensional porous structure of graphene with very thin planes and curly state. Figure 2(b) reveals that nanosized CoO, derived from the decomposition of $Co_4(CO)_{12}$ cluster and subsequently the oxidation by the oxygen contained in the solutions, firmly adhered to the surface of the graphene substrates or was surrounded by flexible graphene nanosheets, which can preserve the 3-dimensional porous structure of nanosized CoO/ graphene composites.

Figure 2(c) presents a low magnification TEM image of the nanosized CoO/graphene composites. It is observed that nanosized CoO is uniformly and fully distributed on the two-dimensional graphene nanosheets. A high magnification TEM image in Fig. 1(d) reveals that the average particle size of CoO was determined to be 2−4 nm. In this experiment, Co atom was derived

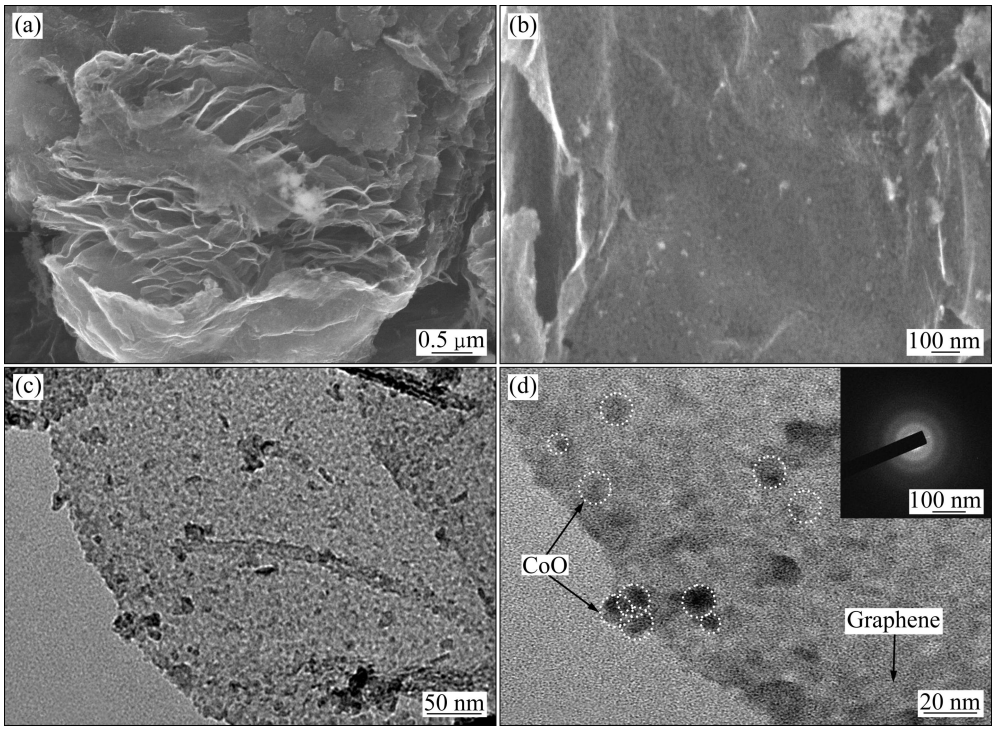

Fig. 2 SEM images (a,b), and TEM images (c,d) of CoO/graphene composites (Inset in (d) is SAED pattern of CoO)

from the decomposition of $Co_4(CO)_{12}$ cluster and then oxidized with the oxygen contained in the solutions during the fast ultrasonic preparation processes at room temperature. Thus a small-sized CoO was formed and firmly adhered to the support of graphene. With the characteristic of the corresponding selected area electron diffraction (SAED) pattern inset in Fig. 2(d), nanosized CoO distributed on the graphene matrix was amorphous due to a fast synthesis at a relative low temperature.

The chemical compositions of nanosized CoO/graphene composites were further investigated by X-photoelectron spectroscopy (XPS) measurements. Full XPS spectrum was firstly employed to determine the existence of all elements in the composites. Figure 3(a) reveals the presence of Co, O and C elements in the composites, which suggests the presence of metal oxides and graphene. The Co 2p XPS spectra of the composites in Fig. 3(b) exhibit two major peaks at 782.7 and 798.2 eV, corresponding to Co $2p_{3/2}$ and Co $2p_{1/2}$, respectively. The spin-energy separation between the peak of Co $2p_{3/2}$ and the peak of Co $2p_{1/2}$ is approximately at 15.5 eV, which is the characteristic of CoO phase, while two small peaks at 787.2 and 803.7 eV are Co^{2+} shake-up satellite peaks of CoO in the composites. The O 1s XPS spectra in Fig. 3(c) show a prominent peak at 532.8 eV and a shoulder peak at 530.8 eV, mainly corresponding to the oxygen species of CoO. And also it reveals that there were few additional residual oxygen-containing groups on the as-prepared graphene. Moreover, the presence of peak at 284.6 eV in Fig. 3(d) was ascribed to the graphitic carbon in graphene, while the C 1s XPS spectra at 288.7 eV, indicate the presence of the oxygen-containing groups in the composites. The above results show that CoO was the prime cobalt oxide phase anchored on the surface of graphene.

The electrochemical performance of the as-prepared CoO/graphene composites was firstly evaluated by galvanostatic charge/discharge cycling at the current density of 50 mA/g. Figure 4(a) shows the charge−discharge profile of the CoO/graphene composites in the 1st, 2nd, 5th, 10th, 20th, 50th cycles. In the first discharge curve, it presents four sloping voltage plateaus: the first sloping voltage plateau presented at ca. 1.5 V but it was absent after several charge/discharge cycles, revealing the existence of the electrochemical reaction between the electrode materials and the electrolytes and the formation of the solid electron layers (SEI) on the surface of the electrode. The following two sloping voltage plateaus at ca. 1.2 and 0.7 V in the discharge profiles and the voltage plateaus at ca. 1.3 and 2.2 V in the charge profiles were ascribed to the lithium insertion/extraction processes in CoO. However, it changed to a long sloping voltage plateau at 1.2−0.7 V and showed a gradual decay in the following charge/discharge processes, indicating some irreversible reaction during the charge/discharge processes due to the amorphous metal oxides in the composites.

Figure 4(b) shows the cycling performance of the CoO/graphene nanohybrids at a current density of 50 mA/g. The CoO/graphene nanohybrids deliver a super

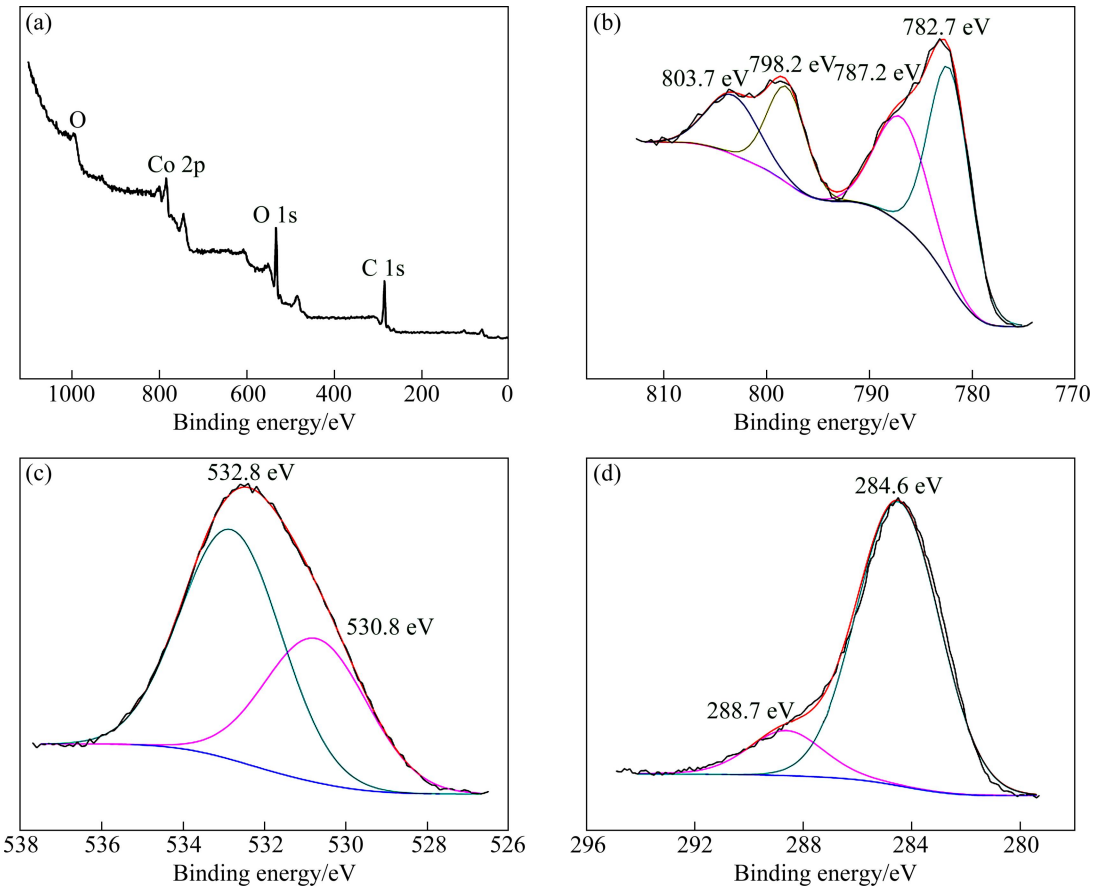

Fig. 3 XPS full spectrum of CoO/graphene composites (a), XPS spectra of Co 2p (b), O 1s (c) and C 2s (d) of CoO/graphene composites

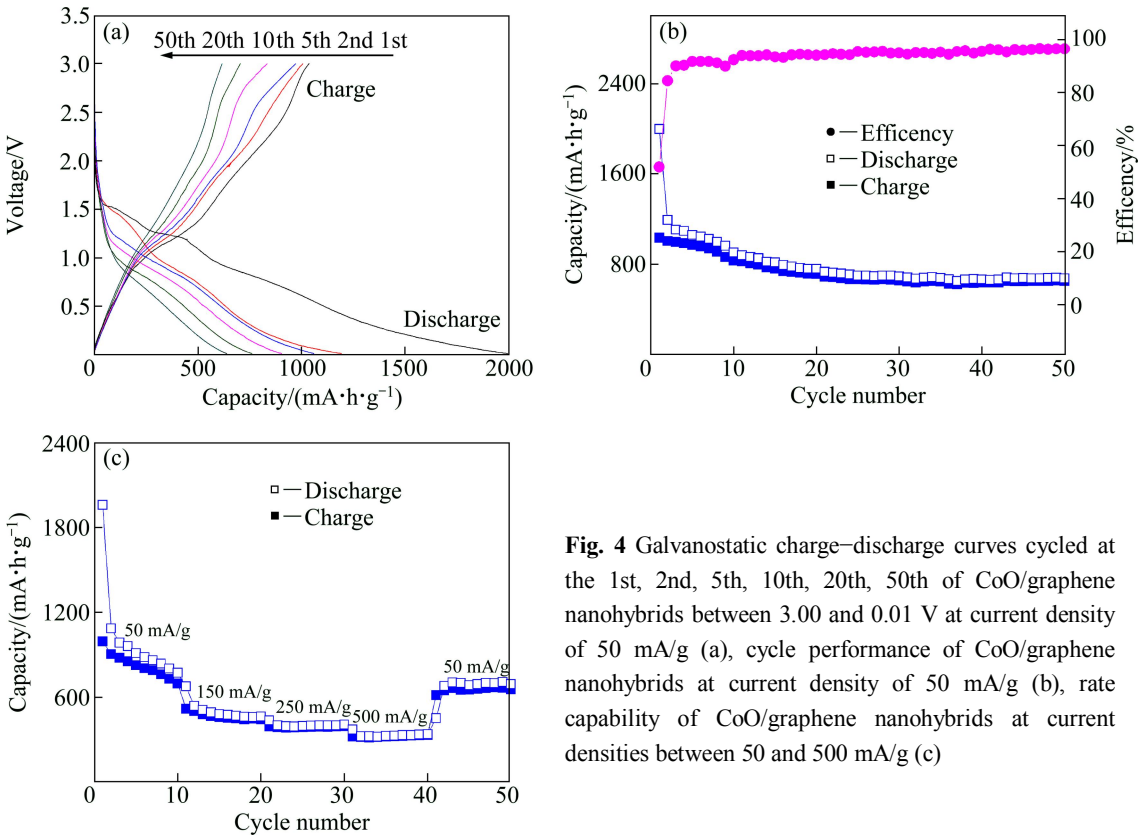

Fig. 4 Galvanostatic charge−discharge curves cycled at the 1st, 2nd, 5th, 10th, 20th, 50th of CoO/graphene nanohybrids between 3.00 and 0.01 V at current density of 50 mA/g (a), cycle performance of CoO/graphene nanohybrids at current density of 50 mA/g (b), rate capability of CoO/graphene nanohybrids at current densities between 50 and 500 mA/g (c)

high lithium storage capacity of 2000 mA·h/g in the first discharge process, which is much higher than the theoretical Li-ion storage capacity of CoO (716 mA·h/g), and also higher than other reported result for CoO/graphene composites [10]. However, a relative low charge capacity of 1036 mA·h/g is achieved, corresponding to a coulombic efficiency of 52%. The large irreversible capacity loss during the first cycle is mainly related to the irreversible lithium loss due to the formation of SEI layer. In the second cycle, a discharge capacity of 1200 mA·h/g is achieved and the coulombic efficiency increases to 85%. The capacitance continuously decreases over the first 20 cycles and becomes stable in subsequent cycles. The capacitance retention is more than 95% after 50 cycles and the reversible capacity of the CoO/graphene nanohybrids reaches 650 mA·h/g, almost twice that of commercial graphite anode, demonstrating the high lithium storage capability and the excellent cycling behavior of the sample.

Figure 4(c) shows the specific charge capacity of the CoO/graphene nanohybrids as a function of cycle number and current density. As shown in Fig. 3(c), the CoO/graphene nanohybrids show a reversible capacity of 700 mA·h/g after the 10th cycle at a current density of 50 mA·h/g, then 450 mA·h/g after the 20th cycle at 150 mA·h/g, 400 mA·h/g after the 30th cycle at 250 mA·h/g, 340 mA·h/g after the 40th cycle at 500 mA·h/g. A retention of 49% in total is obtained when the current density is enlarged 10 times from 50 to 500 mA·h/g. When the rate returns from 500 mA·h/g to the initial 50 mA·h/g, the electrode charge capacity almost recovers its original value of 650 mA·h/g. The extraordinary performance attributes to the specific structure of the CoO/graphene nanohybrids which offer the good conductivity for Li-ion diffusion and large quantity of accessible sites for Li-ion insertion.

4 Conclusions

1) CoO nanoparticles with average diameter of 3−5 nm homogeneously adhered to the surfaces of graphene via a ultrasonic method.

2) The as-prepared CoO/graphene nanohybrids were used as anode materials for lithium ion battery and the electrode demonstrated extraordinary performance, such as high reversible lithium storage capacity (650 mA·h/g after 50 cycles, almost twice that of commercial graphite anode), high coulombic efficiency (over 95%) and excellent cycling stability.

References

[1] WANG Y, CAO G. Developments in nanostructured cathode materials for high-performance lithium-ion batteries [J]. Advanced Materials, 2008, 20(12): 2251−2269.

[2] LIU C, LI F, MA L P, CHENG H M. Advanced materials for energy storage [J]. Advanced Materials, 2010, 22(8): 28−62.

[3] CHAN C K, PENG H, LIU G, MCILWRATH K, ZHANG X F, HUGGINS R A, CUI Y. High-performance lithium battery anodes using silicon nanowires [J]. Nature Nanotechnology, 2007, 3(1): 31−35.

[4] TARASCON J M, ARMAND M. Issues and challenges facing rechargeable lithium batteries [J]. Nature, 2001, 414: 359−367.

[5] BROWNSON D A C, KAMPOURIS D K, BANKS C, E. An overview of graphene in energy production and storage applications [J]. Journal of Power Sources, 2011, 196(11): 4873−4885.

[6] NOVOSELOV K S, GEIM A K, MOROZOV S V, JIANG D, ZHANG Y, DUBONOS S V, GRIGOUIEVA I V, FIRSOV A A. Electric field effect in atomically thin carbon films [J]. Science, 2004, 306(5696): 666−669.

[7] LUO B, LIU S, ZHI L. Chemical approaches toward graphene-based nanomaterials and their applications in energy-related areas [J]. Small, 2012, 8(5): 630−646.

[8] SUN Y, WU Q, SHI G. Graphene based new energy materials [J]. Energy Environmental Sci, 2011, 4(4): 1113−1132.

[9] WANG X, ZHOU X, YAO K, ZHANG J, LIU Z. A SnO_2/graphene composite as a high stability electrode for lithium ion batteries [J]. Carbon, 2011, 49(1): 133−139.

[10] PENG C, CHEN B, QIN Y, YANG S, LI C, ZUO Y, LIU S, YANG J. Facile ultrasonic synthesis of CoO quantum dot/graphene nanosheet composites with high lithium storage capacity [J]. ACS Nano, 2012, 6(2): 1074−1081.

[11] JI L, TAN Z, KUYKENDALL T R, ALONI S, XUN S, LIN E, BATTAGLIA V, ZHANG Y. Fe_3O_4 nanoparticle-integrated graphene sheets for high-performance half and full lithium ion cells [J]. Physical Chemistry Chemical Physics, 2011, 13(15): 7170−7177.

[12] WU Z S, REN W, WANG D W, LI F, LIU B, CHENG H M. High-energy MnO_2 nanowire/graphene and graphene asymmetric electrochemical capacitors [J]. ACS Nano, 2010, 4(10): 5835−5842.

[13] ZHOU G, WANG D W, YIN L C, LI N, LI F, CHENG H M. Oxygen bridges between NiO nanosheets and graphene for improvement of lithium storage [J]. ACS Nano, 2012, 6(4): 3214−3223.

[14] WANG B, WU X L, SHU C Y, GUO Y G, WANG C R. Synthesis of CuO/graphene nanocomposite as a high-performance anode material for lithium-ion batteries [J]. Journal of Materials Chemistry, 2010, 20(47): 10661−10664.

[15] YANG S, FENG X, MÜLLEN K. Sandwich-like, graphene-based titania nanosheets with high surface area for fast lithium storage [J]. Advanced Materials, 2011, 23(31): 3575−3579.

[16] ZHANG H, XU P, DU G, CHEN Z, OH K, PAN D, JIAO Z. A facile one-step synthesis of tioe/graphene composites for photodegradation of methyl orange [J]. Nano Research, 2011, 4(3): 274−283.

[17] LI S, ZHAO H M, JENA P. Ti-doped nano-porous graphene: A material for hydrogen storage and sensor [J]. Frontiers of Physics in China, 2011, 6(2): 204−208.

[18] WILLIAMS G, KAMAT P V. Graphene-semiconductor nanocomposites: Excited-state interactions between ZnO nanoparticles and graphene oxide [J]. Langmuir, 2009, 25(24): 13869−13873.

[19] WANG H, TIAN H W, WANG X W, QIAO L, WANG S M, WANG X L, ZHENG W T, LIU Y C. Electrical conductivity of alkaline-reduced graphene oxide [J]. Chemical Research in Chinese University, 2011, 27(5): 857−861.

[20] NOVOSELOV K S, JIANG D, SCHEDIN F, BOOTH T J, KHOTKEVICH V V, MOROZOV S V, GEIM A K. Two-dimensional atomic crystals [J]. Proceedings of the National Academy of Sciences of the United States of America, 2005, 102(30): 10451−10453.

[21] NOVOSELOV K S, GEIM A K, MOROZOV S V, JIANG D, GRIGORIEVA M I K I V, DUBONOS S V, FIRSOV A A. Two-dimensional gas of massless Dirac fermions in graphene [J]. Nature, 2005, 438(7065): 197−200.
[22] GEIM A K. Graphene: Status and prospects [J]. Science, 2009, 324(5934): 1530−1534.
[23] ZHOU G, WANG D W, LI F, ZHANG L, LI N, WU Z S, WEN L, LU G Q, CHENG H M. Graphene-wrapped Fe_3O_4 anode material with improved reversible capacity and cyclic stability for lithium ion batteries [J]. Chemistry of Materials, 2010, 22(18): 5306−5313.
[24] WU Z S, REN W, WEN L, GAO L, ZHAO J, CHEN Z, ZHOU G, LI F, CHENG H M. Graphene anchored with Co_3O_4 nanoparticles as anode of lithium ion batteries with enhanced reversible capacity and cyclic performance [J]. ACS Nano, 2010, 4(6): 3187−3194.
[25] WANG H, CUI L F, YANG Y, SANCHEZ C H, ROBINSON J T, LIANG Y, CUI Y, DAI H, Mn_3O_4−graphene hybrid as a high-capacity anode material for lithium ion batteries [J]. Journal of the American Chemical Society, 2010, 132(40): 13978−13980.

高性能锂离子电池负极材料 CoO/石墨烯纳米复合结构的超声法制备

陈炳地[1,2]，彭成信[1,2]，崔 征[2]

1. 同济大学 材料科学与工程学院，上海 201804；
2. 同济大学 医学院 先进材料与纳米生物医学研究院，上海 200092

摘 要：以羰基钴为原料，采用简易超声法制备氧化亚钴和石墨烯纳米复合结构。通过扫描电子显微镜(SEM)、透射电子显微镜(TEM)及光电子能谱(XPS)对该纳米复合结构进行表征。结果表明：粒径为 3~5 nm 的氧化亚钴纳米颗粒均匀分布于石墨烯表面。将氧化亚钴/石墨烯纳米复合结构用作锂离子电池负极材料，电化学测试结果表明，该复合结构具有高电容量(50 次循环后电容量为 650 mA·h/g，约是商用石墨电极的 2 倍)、高库伦效率(高于 95%)以及很好的循环稳定性。该优异的电化学性能源于氧化亚钴/石墨烯纳米复合结构的特点：纳米尺寸的氧化亚钴颗粒分散于导电的石墨烯衬底上，有利于锂离子的嵌入和脱嵌，缩短了锂离子的扩散路径，提高了氧化物的导电性，从而改善了材料的电性能。

关键词：锂离子电池；石墨烯；氧化亚钴；负极材料；超声制备

(Edited by LI Xiang-qun)